Get set. Go! ...

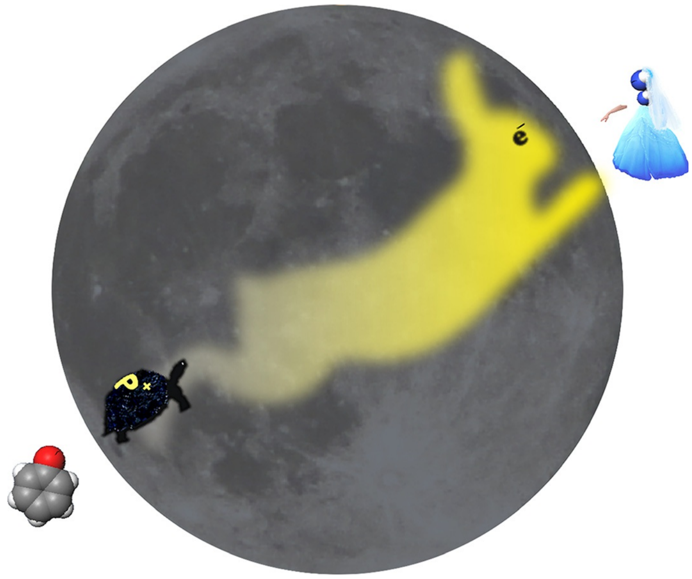

… The excited-state hydrogen atom transfer of a phenol-(ammonia)$_5$ hexamer is like a race. In their Communication on page 15089 ff. C. Jouvet, M. Fujii et al. show by time-resolved spectroscopy that an electron jumps like a hare, reaching the solvent “princess” within 3 picoseconds of photoexcitation and leaving its partner, a proton, behind. The proton moves slowly but steadily like a tortoise, and finally reaches the princess after 15 picoseconds.

Amine Alkylation

In their Communication on page 15046 ff., R. Kempe et al. describe the alkylation of amines by alcohols in the presence of a Co catalyst under mild conditions. Selectively monoalkylated aromatic amines as well as unsymmetrically substituted diamines are obtained.

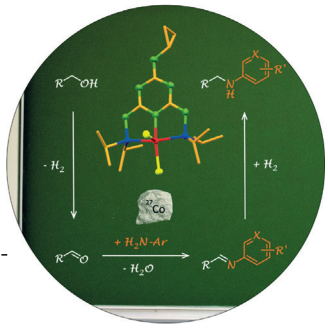

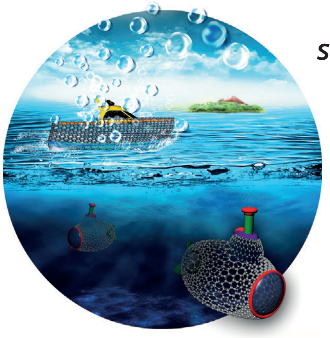

Superabsorbers

Wrinkled graphene monoliths were used as building blocks for the on-demand construction of superhydrophobic or superhydrophilic films on arbitrary substrates by J.-S. Chen, X.-H. Li et al., as described in their Communication on page 15165 ff.

Liquid Crystals

In their Communication on page 15266 ff., S.-H. Kim et al. describe the synthesis of reconfigurable photonic microcapsules through microfluidic encapsulation of cholesteric liquid crystals with a double layer.

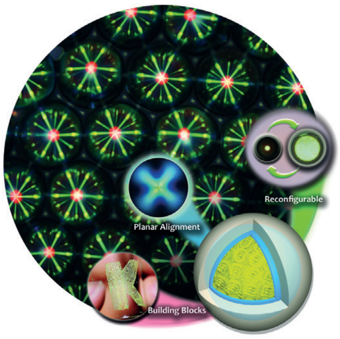

How to contact us:

Editorial Office:
E-mail: angewandte@wiley-vch.de
Fax: (+49) 6201–606-331
Telephone: (+49) 6201–606-315

Reprints, E-Prints, Posters, Calendars:
Carmen Leitner
E-mail: chem-reprints@wiley-vch.de
Fax: (+49) 6201–606-331
Telephone: (+49) 6201–606-327

Copyright Permission:
Bettina Loycke
E-mail: rights-and-licences@wiley-vch.de
Fax: (+49) 6201–606-332
Telephone: (+49) 6201–606-280

Online Open:
Margitta Schmitt
E-mail: angewandte@wiley-vch.de
Fax: (+49) 6201–606-331
Telephone: (+49) 6201–606-315

Subscriptions:
www.wileycustomerhelp.com
Fax: (+49) 6201–606-184
Telephone: 0800 1800536 (Germany only)
+44(0) 1865476721 (all other countries)

Advertising:
Marion Schulz
E-mail: mschulz@wiley-vch.de
Fax: (+49) 6201–606-550
Telephone: (+49) 6201–606-565

Courier Services:
Boschstrasse 12, 69469 Weinheim

Regular Mail:
Postfach 101161, 69451 Weinheim

Angewandte Chemie International Edition is a journal of the Gesellschaft Deutscher Chemiker (GDCh), the largest chemistry-related scientific society in continental Europe. Information on the various activities and services of the GDCh, for example, cheaper subscription to *Angewandte Chemie International Edition*, as well as applications for membership can be found at **www.gdch.de** or can be requested from GDCh, Postfach 900440, D-60444 Frankfurt am Main, Germany.

GDCh
GESELLSCHAFT DEUTSCHER CHEMIKER

© 2015 Wiley-VCH Verlag GmbH & Co. KGaA, Weinheim

Get the Angewandte App International Edition

Available on the App Store

Enjoy Easy Browsing and a New Reading Experience on the iPad or iPhone
- Keep up to date with the latest articles in Early View.
- Download new weekly issues automatically when they are published.
- Read new or favorite articles anytime, anywhere.

Editorial

Service

Author Profile

Books

News


J. A. Prescher


B. L. Pentelute


W. Kroutil


H. J. Wörner

Minireviews

Surface Structuring

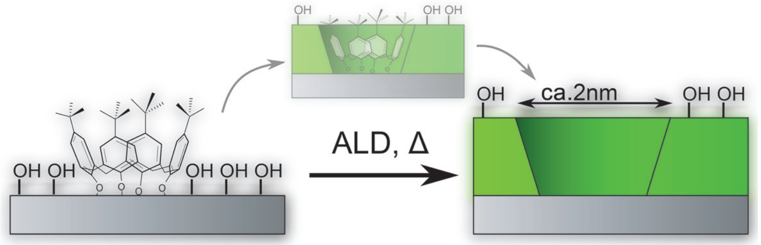

Deposit account: Atomic layer deposition (ALD) has great potential for the nanoscale structuring of surfaces. This Minireview highlights the application of ALD to the structuring of both planar and porous materials. The nanoscale structuring of high-surface-area materials by ALD is now even feasible, thus enabling novel applications, such as those in the fields of catalysis and alternative energy.

Reviews

Organogold Chemistry

Sitting on a gold mine? In the past few years, the reactivity of gold complexes has been extended well beyond Lewis acid behavior and electrophilic activation of π-substrates. Elementary steps considered highly unlikely, if not impossible, for gold complexes have been unambiguously demonstrated, offering new perspectives in gold catalysis.

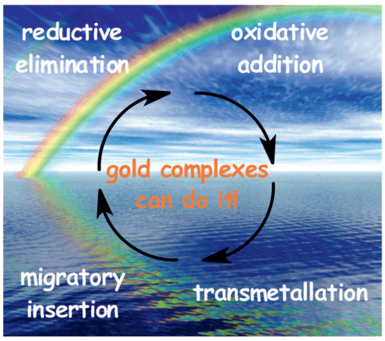

For the USA and Canada:
ANGEWANDTE CHEMIE International Edition (ISSN 1433-7851) is published weekly by Wiley-VCH, PO Box 101161, 69451 Weinheim, Germany. US mailing agent: SPP, PO Box 437, Emigsville, PA 17318. Periodicals postage paid at Emigsville, PA. US POSTMASTER: send address changes to *Angewandte Chemie*, John Wiley & Sons Inc., C/O The Sheridan Press, PO Box 465, Hanover, PA 17331. Annual subscription price for institutions: US$ 11.738/10.206 (valid for print and electronic / print or electronic delivery); for individuals who are personal members of a national chemical society prices are available on request. Postage and handling charges included. All prices are subject to local VAT/sales tax.

Communications

Amine Alkylation

S. Rösler, M. Ertl, T. Irrgang, R. Kempe* ———— 15046 – 15050

Cobalt-Catalyzed Alkylation of Aromatic Amines by Alcohols

Frontispiece

Sustainable C–N bond formation: An easily accessible Co complex efficiently catalyzes the alkylation of aromatic amines by alcohols. The mild reaction conditions permit the use of sensitive functional groups (I, Br) and the observed selective monoalkylation allows the synthesis of unsymmetrically alkylated diamines.

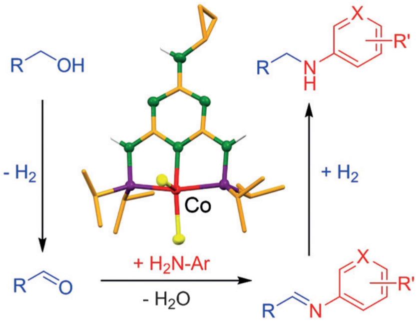

Enantioselective N-Dealkylation

S. Gandomkar, E.-M. Fischereder, J. H. Schrittwieser, S. Wallner, Z. Habibi, P. Macheroux, W. Kroutil* ———— 15051 – 15054

Enantioselective Oxidative Aerobic Dealkylation of *N*-Ethyl Benzylisoquinolines by Employing the Berberine Bridge Enzyme

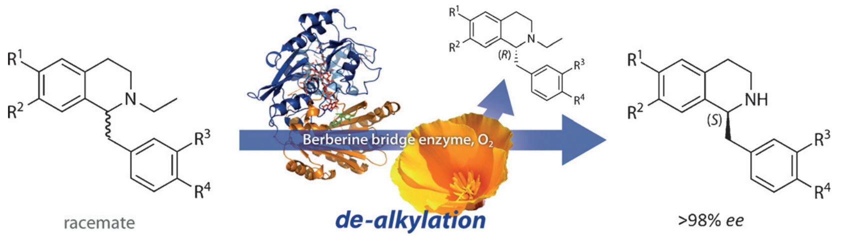

Flower power: *N*-Ethyl-substituted 1-benzyl-1,2,3,4-tetrahydroisoquinoline derivatives were enantioselectively dealkylated in a reaction mediated by promiscuous activity of the berberine bridge enzyme, a C–C bond forming enzyme originating from the California poppy.

Chemical Ligation

S. F. Loibl, Z. Harpaz, O. Seitz* ———— 15055 – 15059

A Type of Auxiliary for Native Chemical Peptide Ligation beyond Cysteine and Glycine Junctions

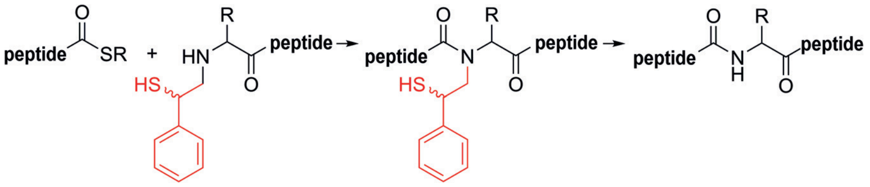

A radical change of the auxiliary design enables extended native chemical peptide ligation at sterically demanding ligation junctions. The 2-mercapto-2-phenethyl group is small and flexible and avoids α-branching. The auxiliary is introduced by reductive amination on a solid support and removed under mildly basic conditions in a radical desulfurization triggered fragmentation reaction.

Main-Group-Element Chemistry

K. Hansen, T. Szilvási, B. Blom, M. Driess* ———— 15060 – 15063

A Persistent 1,2-Dihydrophosphasilene Adduct

Closer to the roots: 1,2-Dihydrophosphasilene derivative **1** could be synthesized from the corresponding arylchlorosilylene–N-heterocyclic carbene (NHC) adduct and $LiPH_2$ and is stabilized by NHC→Si donor–acceptor complexation. Remarkably, the Si–P double-bond character in **1** is more like the betain-like resonance form **1′**.

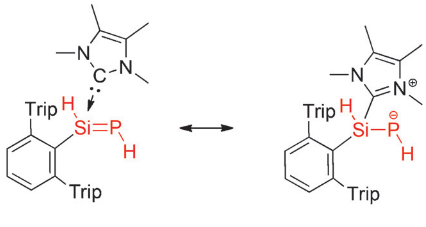

1 **1'**

© 2015 Wiley-VCH Verlag GmbH & Co. KGaA, Weinheim

DNA Immobilization

D. Jambrec, M. Gebala, F. La Mantia,
W. Schuhmann* ________ 15064 – 15068

Potential-Assisted DNA Immobilization as a Prerequisite for Fast and Controlled Formation of DNA Monolayers

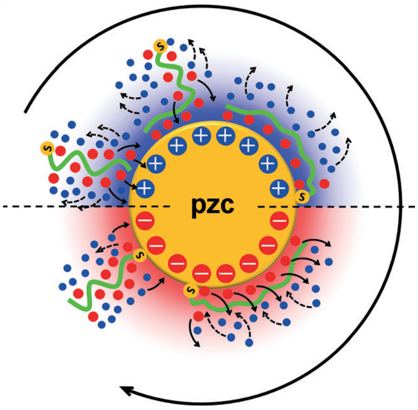

Stir it up: The desired DNA coverage can be reached within minutes by stirring the DNA in front of an electrode by means of a pulse-type potential modulation. The mechanism of potential-assisted immobilization can be understood by considering the role of ions surrounding the DNA, the distance over which applied potentials have an impact on DNA, and the shift of the potential of zero charge (pzc) during the immobilization due to DNA immobilization.

Biomineralization

A. Jantschke, E. Koers, D. Mance,
M. Weingarth, E. Brunner,*
M. Baldus* ________ 15069 – 15073

Insight into the Supramolecular Architecture of Intact Diatom Biosilica from DNP-Supported Solid-State NMR Spectroscopy

Heart of glass: A DNP-supported ssNMR approach assisted by microscopy, mass spectrometry, and molecular dynamics simulations was applied to study the structural organization of intact biosilica. First insight into the in situ secondary structure elements of tightly biosilica-associated native proteins was obtained. Based on the results, a novel model for the location and supramolecular arrangement of intact biosilica is suggested.

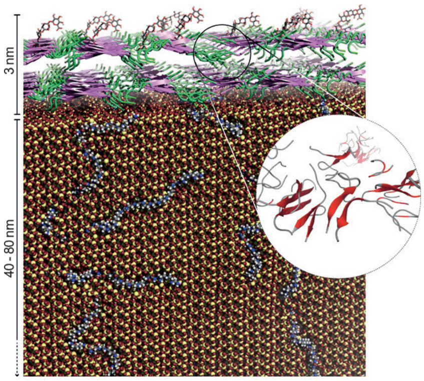

BN-Heterocycles

S. Wang,* D.-T. Yang, J. Lu,
H. Shimogawa, S. Gong,* X. Wang,
S. K. Mellerup, A. Wakamiya, Y.-L. Chang,
C. Yang, Z.-H. Lu* ________ 15074 – 15078

In Situ Solid-State Generation of $(BN)_2$-Pyrenes and Electroluminescent Devices

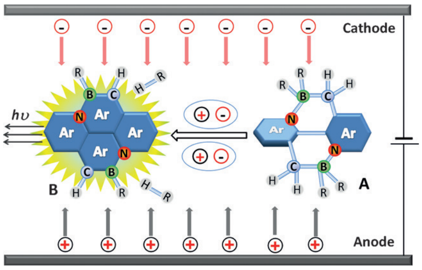

Arene elimination reactions of BN-heterocycles (**A**) in an electroluminescent device result in the in situ formation of BN-pyrenes (**B**) and BN-phenanthrenes. This is a novel approach to the creation of functional EL devices.

Drug Discovery

T. Rodrigues, D. Reker, M. Welin,
M. Caldera, C. Brunner, G. Gabernet,
P. Schneider, B. Walse,
G. Schneider* ________ 15079 – 15083

De Novo Fragment Design for Drug Discovery and Chemical Biology

Automated computational molecular design generated a fragment-sized inhibitor of death-associated protein kinase 3, which was confirmed by X-ray crystallography of the kinase–inhibitor complex. Target prediction software identified additional macromolecular targets of the designed compound and the structurally closely related drug azosemide.

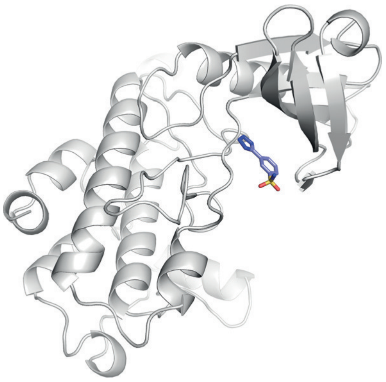

© 2015 Wiley-VCH Verlag GmbH & Co. KGaA, Weinheim

Main-Group Chemistry

T. Kupfer, H. Braunschweig,*
K. Radacki ______ **15084 – 15088**

The Triboracyclopropenyl Dianion: The Lightest Possible Main-Group-Element Hückel π Aromatic

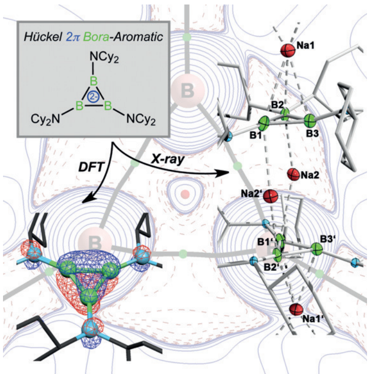

Chemical reduction of Cl$_2$BNCy$_2$ afforded Na$_4$[B$_3$(NCy$_2$)$_3$]$_2$·2 DME, which contains the triboracyclopropenyl dianion [B$_3$(NCy$_2$)$_3$]$^{2-}$, a boron-based analogue of the prototypical Hückel 2π aromatic [C$_3$H$_3$]$^+$. Both X-ray diffraction and density functional theory are indicative of B–B multiple bonding and the presence of a cyclically delocalized 2π electron system.

Hydrogen Transfer

M. Miyazaki, R. Ohara, K. Daigoku,
K. Hashimoto, J. R. Woodward,
C. Dedonder, C. Jouvet,*
M. Fujii* ______ **15089 – 15093**

Electron–Proton Decoupling in Excited-State Hydrogen Atom Transfer in the Gas Phase

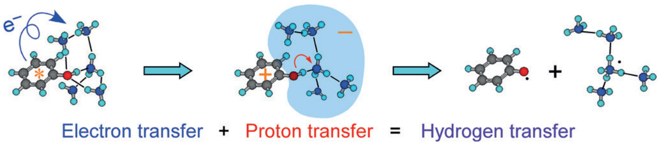

After you: Do the hydrogen nucleus (proton) and electron move together or sequentially in excited-state hydrogen transfer (ESHT)? Time-resolved spectroscopic changes can distinguish between the electron and proton movements in a molecular cluster of phenol solvated by five ammonia molecules. The measurement shows for the first time that the electron moves first and the proton then follows on a much slower timescale.

Front Cover

Phase Transitions

S. Kim, K. W. Nam, S. Lee, W. Cho,
J.-S. Kim, B. G. Kim, Y. Oshima, J.-S. Kim,
S.-G. Doo, H. Chang, D. Aurbach,*
J. W. Choi* ______ **15094 – 15099**

Direct Observation of an Anomalous Spinel-to-Layered Phase Transition Mediated by Crystal Water Intercalation

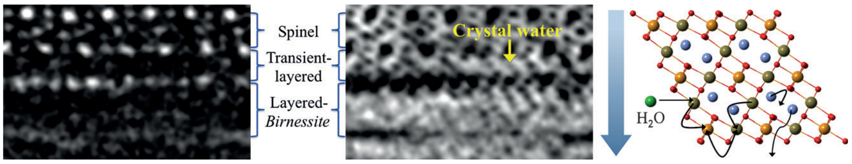

Reversing a phase transition with water: An anomalous spinel-to-layered phase transition is tracked on the atomic scale using scanning transmission electron microscopy. The phase transition is mediated by formation of a transition phase at the phase boundary that traps crystal water in a stepwise manner.

Host–Guest Systems

A. B. Grommet, J. L. Bolliger, C. Browne,
J. R. Nitschke* ______ **15100 – 15104**

A Triphasic Sorting System: Coordination Cages in Ionic Liquids

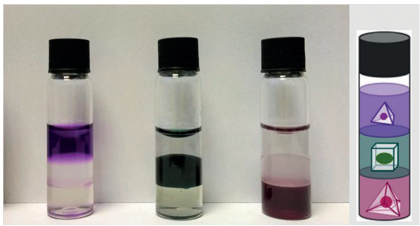

All sorted: In ionic-liquid solutions, coordination cages were shown to be stable and capable of selectively encapsulating guests. A triphasic sorting system was designed, comprising water and two mutually immiscible hydrophobic ionic liquids, such that three different coordination cages were each soluble in a single layer. Upon addition of a mixture of three different guests, each cage bound its preferred guest.

© 2015 Wiley-VCH Verlag GmbH & Co. KGaA, Weinheim

Drug Delivery

S. Schmidt, M. J. W. Adjobo-Hermans,
R. Wallbrecher, W. P. R. Verdurmen,
P. H. M. Bovée-Geurts, J. van Oostrum,
F. Milletti, T. Enderle,
R. Brock* ______ 15105 – 15108

Detecting Cytosolic Peptide Delivery with the GFP Complementation Assay in the Low Micromolar Range

Peptide-based GFP complementation: Cells expressing the GFP1-10 GFP fragment (gray circle) are electroporated or penetrated with GFP-11 (gray squares) conjugated by a linker (blue line) to a cell-penetrating peptide (orange line), thereby resulting in delivery into the cytosol and GFP complementation and fluorescence (green circle).

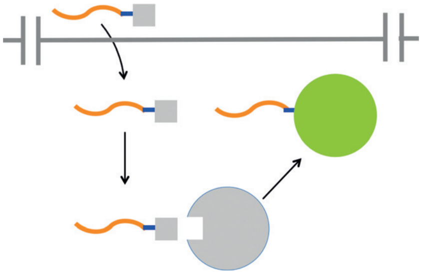

Solid-Phase Synthesis

G. Serghiou,* G. Ji, N. Odling,
H. J. Reichmann, J.-P. Morniroli,
R. Boehler, D. J. Frost, J. P. Wright,
B. Wunder ______ 15109 – 15112

Creating Reactivity with Unstable Endmembers using Pressure and Temperature: Synthesis of Bulk Cubic $Mg_{0.4}Fe_{0.6}N$

Exploiting instability: The new nitride phase $Mg_{0.4}Fe_{0.6}N$ is formed by removing MgN and FeN endmember lattice mismatch with pressure to allow a stabilizing redistribution of valence electrons upon heating. The reasons for cubic endmember nitride instability become the driving force for cubic nitride solid solution stability.

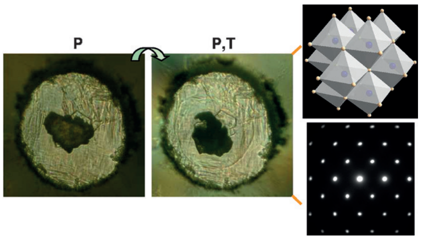

Water Splitting

S. M. Lang,* T. M. Bernhardt, D. M. Kiawi,
J. M. Bakker,* R. N. Barnett,
U. Landman* ______ 15113 – 15117

The Interaction of Water with Free $Mn_4O_4^+$ Clusters: Deprotonation and Adsorption-Induced Structural Transformations

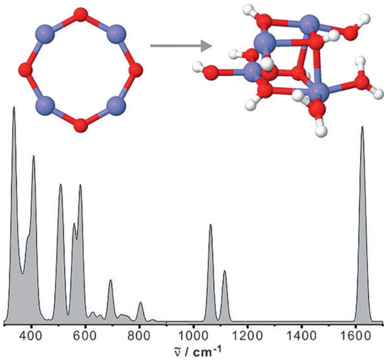

Be natural and flexible! Manganese oxide is one of the materials of choice in the quest for versatile, earth-abundant water-splitting catalysts. Employing free clusters as molecular model systems provides fundamental insight into the deprotonation of water. First-principles calculations in conjunction with vibrational spectroscopy reveal a structural transformation of the cluster induced by the one-by-one adsorption and deprotonation of H_2O molecules.

DNA Nanotechnology

H. Zuo,* S. Wu, M. Li, Y. Li, W. Jiang,
C. Mao* ______ 15118 – 15121

A Case Study of the Likes and Dislikes of DNA and RNA in Self-Assembly

Inside Cover

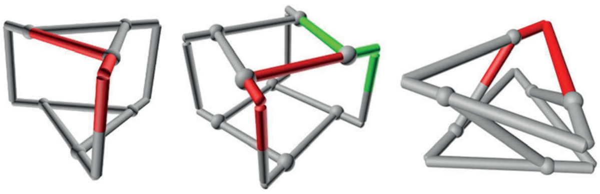

The composition of a nucleic acid nanomotif (RNA or DNA) has a significant influence on its structure. DNA motifs with certain single-stranded loops and tails yielded triangular prisms (see scheme, left and right) whereas two complementary motifs need to be combined to obtain tetragonal prisms (middle).

© 2015 Wiley-VCH Verlag GmbH & Co. KGaA, Weinheim

Amphiphiles

P. M. Erne, L. S. van Bezouwen, P. Štacko, D. J. van Dijken, J. Chen, M. C. A. Stuart, E. J. Boekema, B. L. Feringa* ———— 15122 – 15127

Loading of Vesicles into Soft Amphiphilic Nanotubes using Osmosis

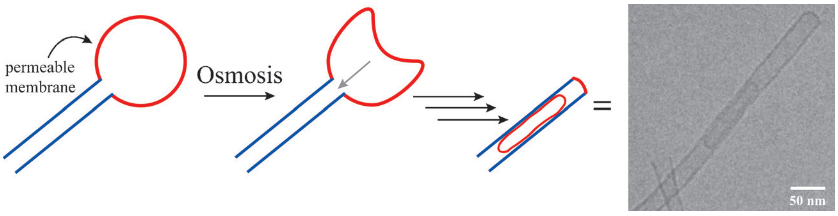

Inspired by nature: The osmotically induced shape change of a vesicle attached to the end of a rigid amphiphilic nanotube is used in combination with geometrical constraints to load a vesicle inside the nanotube. A low salt gradient between the inside and outside of the nanotube is sufficient to induce inclusion of vesicles.

Oligoribonucleotides

M. Košutić, S. Neuner, A. Ren, S. Flür, C. Wunderlich, E. Mairhofer, N. Vušurović, J. Seikowski, K. Breuker, C. Höbartner, D. J. Patel,* C. Kreutz,* R. Micura* ———— 15128 – 15133

A Mini-Twister Variant and Impact of Residues/Cations on the Phosphodiester Cleavage of this Ribozyme Class

Efficient cleavage of the twister ribozyme class does not require the phylogenetically conserved stem P1. The shifted pK_a of the adenine at the cleavage site together with Mn^{2+}- or Cd^{2+}-accelerated cleavage of S_P phosphorothioate substrates suggest the combination of nucleobase-assisted acid–base catalysis and metal-ion catalysis.

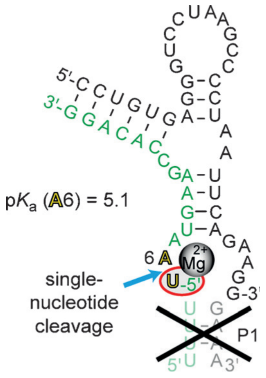

Electrochemistry

R. Chen, N. Nioradze, P. Santhosh, Z. Li, S. P. Surwade, G. J. Shenoy, D. G. Parobek, M. A. Kim, H. Liu, S. Amemiya* ———— 15134 – 15137

Ultrafast Electron Transfer Kinetics of Graphene Grown by Chemical Vapor Deposition

Large-area graphene grown by chemical vapor deposition shows very high electrochemical reactivity when polystyrene is employed for electrode fabrication instead of the conventional poly(methyl methacrylate). Ultrafast oxidation of ferrocenemethanol (FcMeOH) is monitored by nanogap voltammetry based on scanning electrochemical microscopy, yielding unprecedentedly high standard electron-transfer rate constants ($k^0 \geq 25\ cm\,s^{-1}$).

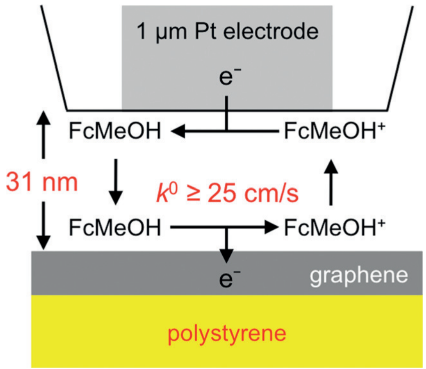

Proton Storage

S. S. Nadif, M. E. O'Reilly, I. Ghiviriga, K. A. Abboud, A. S. Veige* ———— 15138 – 15142

Remote Multiproton Storage within a Pyrrolide-Pincer-Type Ligand

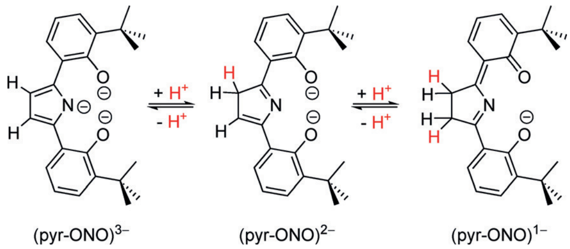

State of play: A pyrrole-centered pincer ligand (pyr-ONO) has been synthesized that can switch from a monoanionic state to a trianionic state through reversible remote protonation (see scheme). Combining two ligands within one metal coordination sphere and subsequent protonation allows remote storage of a total of three protons.

Surface Chemistry

C. Rogers, C. Chen, Z. Pedramrazi,
A. A. Omrani, H.-Z. Tsai, H. S. Jung, S. Lin,
M. F. Crommie,*
F. R. Fischer* ________ **15143 – 15146**

Closing the Nanographene Gap: Surface-Assisted Synthesis of Peripentacene from 6,6′-Bipentacene Precursors

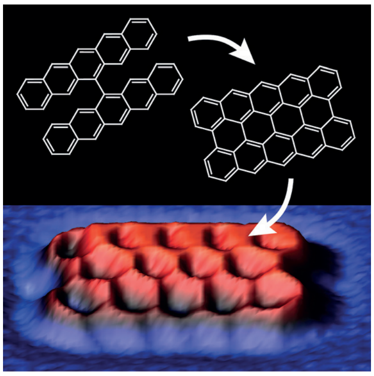

Zip it up: Synthesis and atomic-resolution non-contact AFM imaging of a surface-stabilized peripentacene is reported. The key intermediate is the metastable 6,6-bipentacene precursor, which was obtained through a Staudinger-type diazo-thioketone coupling followed by selective 1,4-elimination.

Natural Products Synthesis

H. Wada, H. E. L. Williams,
C. J. Moody* ________ **15147 – 15151**

Total Synthesis of the Posttranslationally Modified Polyazole Peptide Antibiotic Plantazolicin A

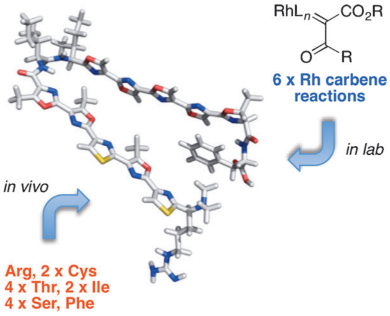

You can count on carbenes: The power of the rhodium carbene methodology is demonstrated by a new synthesis of the polyazole antibiotic plantazolicin A. Rhodium(II)-catalyzed reactions of diazo-carbonyl compounds were used to generate several of the seven oxazole rings in the natural product. NMR spectroscopy and molecular modeling revealed a likely dynamic hairpin conformation with two isoleucine residues in the hinge region (see picture).

Nanomaterials

I. Roy, D. Shetty, R. Hota, K. Baek, J. Kim,
C. Kim, S. Kappert,
K. Kim* ________ **15152 – 15155**

A Multifunctional Subphthalocyanine Nanosphere for Targeting, Labeling, and Killing of Antibiotic-Resistant Bacteria

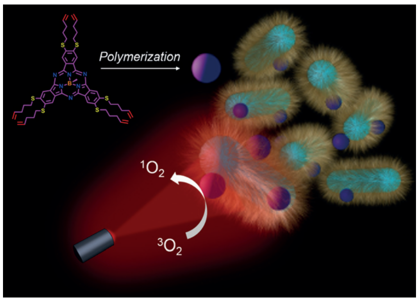

Killing me softly: A multifunctional, water-dispersible nanosphere composed of covalently linked subphthalocyanine units was synthesized. The nanosphere can target, label, and photoinactivate antibiotic-resistant bacteria with exceptional efficiency even at a low dosage. The nanomaterial also shows promise in photoacoustic imaging of bacteria in vivo.

Protein Thermal Stability

M. J. Edgeworth, J. J. Phillips, D. C. Lowe,
A. D. Kippen, D. R. Higazi,
J. H. Scrivens* ________ **15156 – 15159**

Global and Local Conformation of Human IgG Antibody Variants Rationalizes Loss of Thermodynamic Stability

A combination of ion-mobility mass spectrometry (IM-MS) and hydrogen/deuterium exchange mass spectrometry (HDX-MS) approaches were used to elucidate the global and local conformation and dynamics of engineered IgG Fc variants with reduced thermodynamic stability.

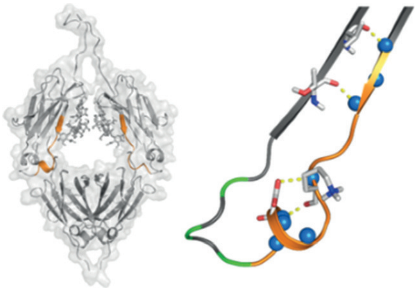

© 2015 Wiley-VCH Verlag GmbH & Co. KGaA, Weinheim

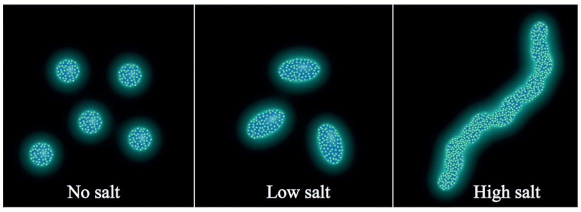

Seeing is believing: The direct visualization of micelle transitions is usually prevented by aggregation-induced quenching of light emission in the micelle solution. The use of a surfactant with a tetraphenylethene core and aggregation-induced emission characteristics enabled fluorescence monitoring of the transition of micelles from spherical to rodlike and wormlike structures as the salt concentration of the solution increased (see picture).

Fluorescent Micelles

W. Guan, W. Zhou, C. Lu,*
B. Z. Tang* ______ 15160 – 15164

Synthesis and Design of Aggregation-Induced Emission Surfactants: Direct Observation of Micelle Transitions and Microemulsion Droplets

---

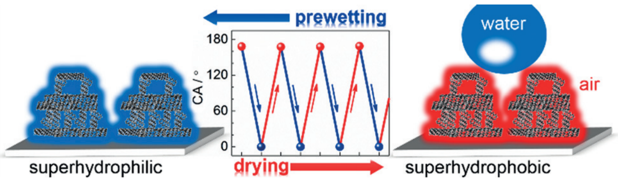

Rapid changes: Superabsorbing graphene monoliths with wrinkled surfaces were dispersed in water or other common solvents to obtain paintable inks for constructing rough surfaces on arbitrary substrates. These surfaces are either superhydrophobic or superhydrophilic depending on the adsorbed layer (air and water, respectively) and can be reversibly switched simply by prewetting with ethanol and drying in air.

Superabsorbers

L.-B. Lv, T.-L. Cui, B. Zhang, H.-H. Wang,
X.-H. Li,* J.-S. Chen* ______ 15165 – 15169

Wrinkled Graphene Monoliths as Superabsorbing Building Blocks for Superhydrophobic and Superhydrophilic Surfaces

Inside Back Cover

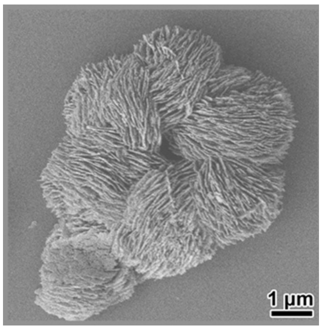

Chiral inorganic materials: ZnO films (see picture) were deposited on quartz substrates using L/D-methionine as both a structure-directing and symmetry-breaking agent. Three levels of hierarchical chirality were studied in the ZnO films. The multiple optical activities of these films were attributed to electronic transitions, photoluminescent emission, and Raman scattering.

Chirality

Y. Duan, L. Han, J. Zhang, S. Asahina,
Z. Huang, L. Shi, B. Wang, Y. Cao, Y. Yao,
L. Ma, C. Wang, R. K. Dukor, L. Sun,
C. Jiang, Z. Tang, L. A. Nafie,
S. Che* ______ 15170 – 15175

Optically Active Nanostructured ZnO Films

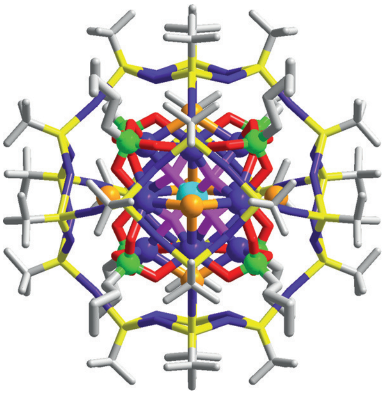

Elaborate Ag–S nanoclusters: Two unprecedented 1D assemblies and an anionic cluster based on silver(I) thiolate cages as their surface components and phosphonate-functionalized silver(I) clusters as cores are reported. The picture shows the outer cationic $[\mathrm{Ag}_{36}(t\mathrm{BuS})_{24}]^{12+}$ cluster that encapsulates the inner anionic $[\mathrm{MoO}_4@\mathrm{Ag}_{12}(n\mathrm{BuPO}_3)_8\mathrm{S}_6]^{18-}$ cluster.

Cage Compounds

Y.-P. Xie,* J.-L. Jin, X. Lu,*
T. C. W. Mak ______ 15176 – 15180

High-Nuclearity Silver Thiolate Clusters Constructed with Phosphonates

Hydrogen Evolution

Z. Huang, W. Luo, L. Ma, M. Yu, X. Ren, M. He, S. Polen, K. Click, B. Garrett, J. Lu, K. Amine, C. Hadad, W. Chen,* A. Asthagiri,* Y. Wu* ____ **15181 – 15185**

Dimeric $[Mo_2S_{12}]^{2-}$ Cluster: A Molecular Analogue of MoS_2 Edges for Superior Hydrogen-Evolution Electrocatalysis

Cutting the edge: A molecular mimic of the MoS_2 edge site, $[Mo_2S_{12}]^{2-}$, has been demonstrated as a superior heterogeneous electrocatalyst for the hydrogen evolution reaction (HER) in acids. Computations suggest that the bridging disulfide ligand of $[Mo_2S_{12}]^{2-}$ exhibits a hydrogen adsorption free energy near zero (−0.05 eV).

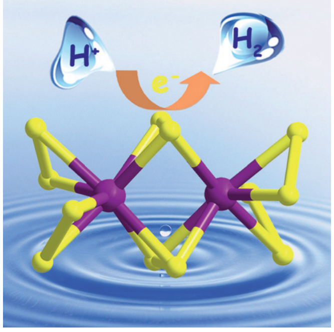

Kinase Activity Assays

X. Zhang, C. Liu,* H. Wang, H. Wang, Z. Li* ____ **15186 – 15190**

Rare Earth Ion Mediated Fluorescence Accumulation on a Single Microbead: An Ultrasensitive Strategy for the Detection of Protein Kinase Activity at the Single-Cell Level

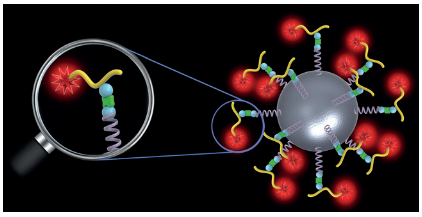

Dy-ing to measure kinases: An ultrasensitive single microbead-based fluorescence imaging (SBFI) strategy is developed for the accurate detection of protein kinase activity. By incorporating rare earth ions, in particular dysprosium, into the phosphopeptide-recognition moiety, protein kinase A activity can be detected down to the single-cell level.

Carbon Nanospheres

G. Wang, Y. Sun, D. Li, H. Liang, R. Dong, X. Feng,* K. Müllen* ____ **15191 – 15196**

Controlled Synthesis of N-Doped Carbon Nanospheres with Tailored Mesopores through Self-Assembly of Colloidal Silica

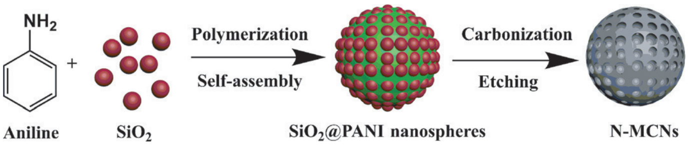

N-doped mesoporous carbon nanospheres (N-MCNs): A highly controlled self-assembly method based on colloidal silica was developed for the facile synthesis of N-MCNs with desired porous and chemical features (tunable mesopore size, high surface area, and N-doping content), which can serve as high-performance electrocatalysts for oxygen reduction reaction.

Porphyrin Wheels

H.-W. Jiang, T. Tanaka, T. Kim, Y. M. Sung, H. Mori, D. Kim,* A. Osuka* ____ **15197 – 15201**

Synthesis of [*n*]Cyclo-5,15-porphyrinylene-4,4′-biphenylenes Displaying Size-Dependent Excitation-Energy Hopping

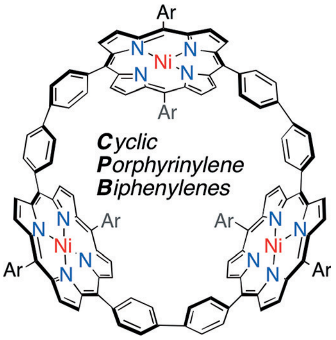

Molecular wheels: A series of 5,15-biphenylene-bridged cyclic porphyrin arrays (see example; Ar = 3,5-*t*$Bu_2C_6H_3$) were obtained by the platination of a 5,15-bis(4-pinacolateboryl)phenyl Ni^{II} porphyrin and subsequent reductive elimination of the Pt^{II}(cod)-bridged cyclic porphyrin intermediates. The ^1H NMR and UV/Vis spectra, redox potentials, and intramolecular excitation-energy-hopping characteristics of the nanorings depend on the ring size.

© 2015 Wiley-VCH Verlag GmbH & Co. KGaA, Weinheim

Enantioselective Catalysis

M. Pappoppula, F. S. P. Cardoso , B. O. Garrett, A. Aponick* ———— 15202 – 15206

Enantioselective Copper-Catalyzed Quinoline Alkynylation

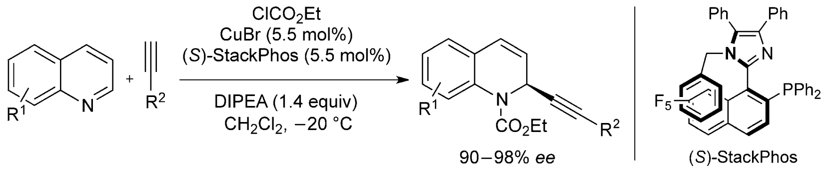

Stacking the deck: Using the axially chiral imidazole-based biaryl, StackPhos, a highly enantioselective copper-catalyzed alkynylation of quinolines has been developed. The method tolerates an unprecedented alkyne scope and both electron-rich and electron-deficient quinolines. Efficient syntheses of the tetrahydroquinoline alkaloids (+)-galipinine, (+)-angustureine, and (−)-cuspareine are reported. DIPEA = diisopropylethylamine.

Carbene Ligands

W. Chen, J. Shen, T. Jurca, C. Peng, Y. Lin, Y. Wang, W. Shih, G. P. A. Yap, T. Ong* ———— 15207 – 15212

Expanding the Ligand Framework Diversity of Carbodicarbenes and Direct Detection of Boron Activation in the Methylation of Amines with CO$_2$

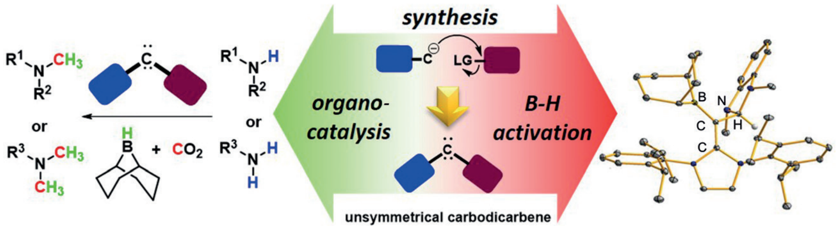

Expanding the family: A simple and convergent synthetic strategy was developed to increase the diversity of the carbodicarbene ligand framework by incorporation of unsymmetrical pendant groups. Reactivity studies revealed that carbodicarbenes are competent organocatalysts for amine methylation using CO$_2$ as a synthon.

Fluorescent Probes

C. Wang, A. Fukazawa,* M. Taki,* Y. Sato, T. Higashiyama,* S. Yamaguchi* ———— 15213 – 15217

A Phosphole Oxide Based Fluorescent Dye with Exceptional Resistance to Photobleaching: A Practical Tool for Continuous Imaging in STED Microscopy

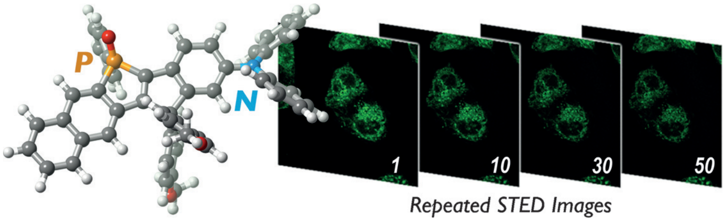

Super photoresistant: The naphthophosphole P-oxide C-Naphox exhibits exceptional resistance to photobleaching and is strongly fluorescent in protic solvents, with large Stokes shifts. This dye is used for continuous imaging in stimulated emission depletion (STED) microscopy. After recording 50 STED images, 83 % of the initial fluorescence intensity persisted.

Asymmetric Amplification

A. Matsumoto,* T. Abe, A. Hara, T. Tobita, T. Sasagawa, T. Kawasaki,* K. Soai* ———— 15218 – 15221

Crystal Structure of the Isopropylzinc Alkoxide of Pyrimidyl Alkanol: Mechanistic Insights for Asymmetric Autocatalysis with Amplification of Enantiomeric Excess

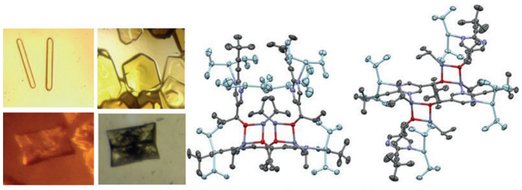

Asymmetric Autocatalyst

One-sided: Single-crystal X-ray diffraction analysis of the isopropyl zinc alkoxide of 5-pyrimidyl alkanol was performed to understand the reaction mechanism of asymmetric autocatalysis. This enabled the elucidation of various aggregate structures considered to be key for the asymmetric amplification.

© 2015 Wiley-VCH Verlag GmbH & Co. KGaA, Weinheim

Electrochromic Devices

K. Qi, J. Wei, M. Sun, Q. Huang, X. Li, Z. Xu, W. Wang,* X. Bai* . **15222 – 15225**

Real-time Observation of Deep Lithiation of Tungsten Oxide Nanowires by In Situ Electron Microscopy

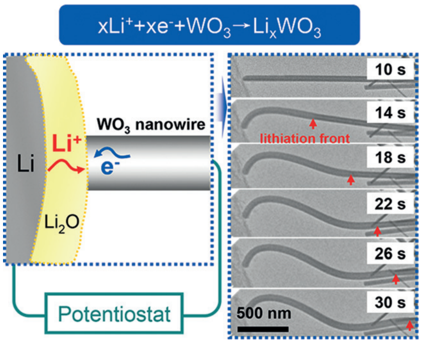

Deep lithiation tracking: The dynamic electrochemical lithiation process of WO_3 nanowires was observed in real time by tracking the structural evolution and reaction forefront during deep lithiation by in situ TEM. These results highlight the chemical and structural flexibility of the Li_xWO_3 phases, and provide insight into the mechanism of WO_3 nanowire lithiation.

Layered Materials

P. Zhou, Q. Xu,* H. Li, Y. Wang,* B. Yan, Y. Zhou, J. Chen, J. Zhang, K. Wang **15226 – 15230**

Fabrication of Two-Dimensional Lateral Heterostructures of $WS_2/WO_3{\cdot}H_2O$ Through Selective Oxidation of Monolayer WS_2

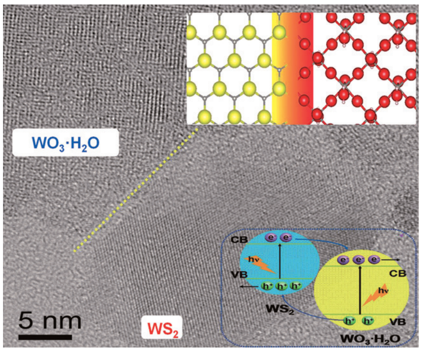

Patchwork: 2D lateral $WS_2/WO_3{\cdot}H_2O$ heterostructures were successfully fabricated through the selective oxidation of monolayer WS_2. The presence of the heterostructures creates long-lived electron–hole pairs, which results in enhanced photocatalytic activity toward the degradation of methyl orange and higher photocurrent under visible-light irradiation.

Light-Emitting Diodes

K. Suzuki, S. Kubo, K. Shizu, T. Fukushima, A. Wakamiya, Y. Murata, C. Adachi, H. Kaji* **15231 – 15235**

Triarylboron-Based Fluorescent Organic Light-Emitting Diodes with External Quantum Efficiencies Exceeding 20%

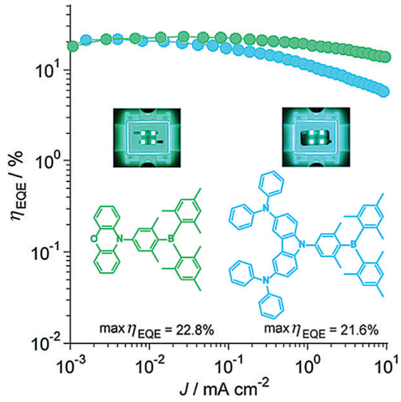

Triarylboron-based emitters are reported that show high photoluminescence quantum yields and efficient up-conversion from triplet to singlet states. Organic light-emitting diodes (OLEDs) using these emitters show a maximum external quantum efficiency of 21.6% for a sky-blue OLED and 22.8% for a green OLED.

Synthetic Methods

G. M. T. Smith, P. M. Burton, C. D. Bray* **15236 – 15240**

Sultones and Sultines via a Julia–Kocienski Reaction of Epoxides

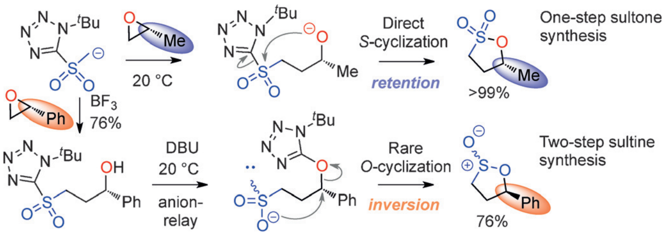

Sultones dance but sultines swing: The development of the homologous Julia–Kocienski reaction has led to the discovery of two new reaction modes of epoxides with sulfones. These pathways allow rapid and direct access to a range of sultones and sultines.

© 2015 Wiley-VCH Verlag GmbH & Co. KGaA, Weinheim

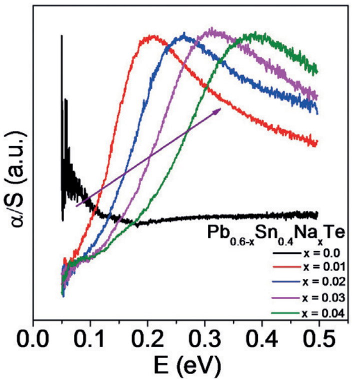

A little sodium changes a lot: Na doping in $Pb_{0.6}Sn_{0.4}Te$ breaks the local crystal mirror symmetry, modifying the electronic structure and widening the electronic band gap. Doping increases p-type carrier concentration and suppresses the bipolar conduction, which together improve the overall thermoelectric properties.

Thermoelectric Materials

S. Roychowdhury, U. S. Shenoy, U. V. Waghmare, K. Biswas* ____ **15241 – 15245**

Tailoring of Electronic Structure and Thermoelectric Properties of a Topological Crystalline Insulator by Chemical Doping

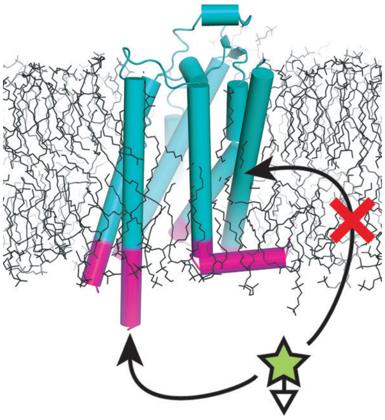

Dyeing of exposure: In-membrane chemical modification (IMCM) enables site-specific labeling of natural cysteine residues in G-protein-coupled receptors with minimal or no mutagenesis by taking advantage of the natural protection of most cysteines by the membrane environment. IMCM is applicable to a wide range of in vitro studies of GPCRs and is a promising platform for in-cell spectroscopy experiments.

Protein Labeling

L. Sušac, C. O'Connor, R. C. Stevens, K. Wüthrich* ____ **15246 – 15249**

In-Membrane Chemical Modification (IMCM) for Site-Specific Chromophore Labeling of GPCRs

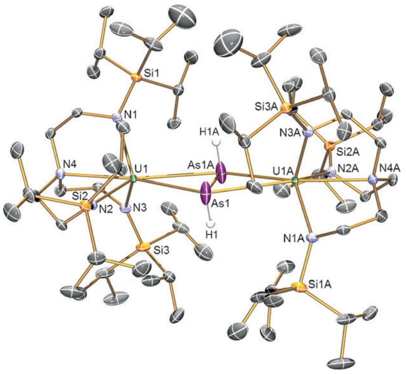

HAsAsH, a molecule first proposed over 200 years ago but never convincingly prepared, has been isolated in a diuranium(IV) complex. Characterization and computational data are consistent with back-bonding-type interactions from uranium to the HAsAsH π*-orbital, thus experimentally confirming the theoretically predicted excellent π-acceptor character of HAsAsH.

Heavy Alkene Analogues

B. M. Gardner, G. Balázs, M. Scheer,* A. J. Wooles, F. Tuna, E. J. L. McInnes, J. McMaster, W. Lewis, A. J. Blake, S. T. Liddle* ____ **15250 – 15254**

Isolation of Elusive HAsAsH in a Crystalline Diuranium(IV) Complex

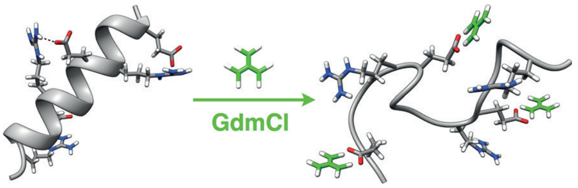

Breaking down the bridges: By investigating α-helical peptides containing different types of salt bridges, the denaturant guanidinium was found to disrupt the folded conformation by breaking salt bridges. Complementary 2-D infrared measurements suggest that denaturation involves binding of guanidinium to the carboxylate groups involved in these salt bridges.

Protein Folding

H. Meuzelaar, M. R. Panman, S. Woutersen* ____ **15255 – 15259**

Guanidinium-Induced Denaturation by Breaking of Salt Bridges

© 2015 Wiley-VCH Verlag GmbH & Co. KGaA, Weinheim

Photocatalytic Nanorods

Y. Liu, B. Zhang, L. Luo, X. Chen, Z. Wang, E. Wu, D. Su, W. Huang* **15260 – 15265**

TiO_2/Cu_2O Core/Ultrathin Shell Nanorods as Efficient and Stable Photocatalysts for Water Reduction

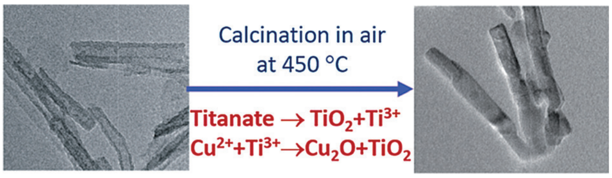

TiO_2/Cu_2O core/ultrathin shell nanorods result in a strong TiO_2–Cu_2O interfacial interaction that facilitates the interfacial charge transfer process and stabilizes the Cu_2O shell, leading to an efficient photocatalyst for water reduction.

Liquid Crystals

S. S. Lee, S. K. Kim, J. C. Won, Y. H. Kim, S.-H. Kim* ______ **15266 – 15270**

Reconfigurable Photonic Capsules Containing Cholesteric Liquid Crystals with Planar Alignment

Back Cover

Photonic microcapsules: Cholesteric liquid crystals (CLCs) are encapsulated by a double layer consisting of an ultrathin alignment layer and an elastic membrane in a microfluidic approach. The alignment layer induces the liquid crystals to adopt a planar alignment, and the elastic membrane renders the microcapsules reconfigurable.

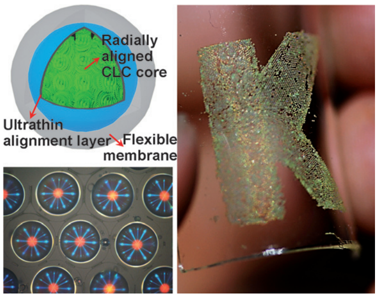

Bifunctional Oxygen Reduction

C. Schiwek, J. Meiners, M. Förster, C. Würtele, M. Diefenbach, M. C. Holthausen,* S. Schneider* ______ **15271 – 15275**

Oxygen Reduction with a Bifunctional Iridium Dihydride Complex

A mononuclear mechanism: The oxygen-reduction reaction (ORR) with an iridium dihydride results in formation of an unusual square-planar iridium(III) hydroxide and water. The dihydride is regenerated with H_2 in a quasi-catalytic synthetic cycle. Experimental and computational studies are in agreement with a four-electron ORR mechanism at a single metal site (see picture).

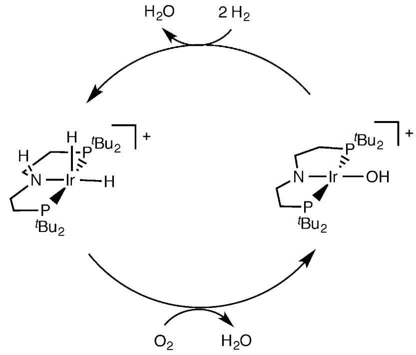

Silylene Dimerization

R. Rodriguez, Y. Contie, Y. Mao, N. Saffon-Merceron, A. Baceiredo,* V. Branchadell, T. Kato* _ **15276 – 15279**

Reversible Dimerization of Phosphine-Stabilized Silylenes by Silylene Insertion into Si^{II}–H and Si^{II}–Cl σ-Bonds at Room Temperature

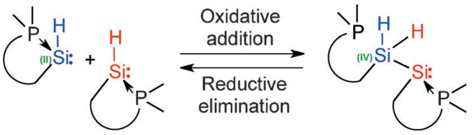

Contrary to the case of classical silylene dimerization to form a disilene, the phosphine-stabilized hydro- and chlorosilylenes undergo a unique dimerization via silylene insertion into the Si–X σ-bond (X = H, Cl), which is reversible at room temperature. DFT calculations indicate that the insertion reaction proceeds in one step in a concerted manner.

© 2015 Wiley-VCH Verlag GmbH & Co. KGaA, Weinheim

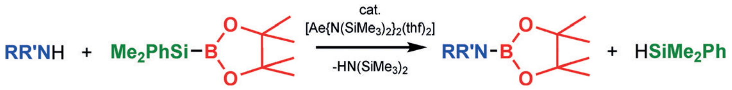

It's a Si→N: Alkaline-earth element (Ae) bis(trimethylsilyl)amides, $[Ae\{N(SiMe_3)_2\}_2(thf)_2]$ (Ae = Mg, Ca, Sr), are precatalysts for boron–nitrogen bond formation through the desilacoupling of amines, RR′NH (R = alkyl, aryl; R′ = H, alkyl, aryl), and $pinBSiMe_2Ph$ (pin = pinacolato; see scheme).

Desilacoupling

D. J. Liptrot, M. Arrowsmith,
A. L. Colebatch, T. J. Hadlington,
M. S. Hill,* G. Kociok-Köhn,
M. F. Mahon ____ **15280 – 15283**

Beyond Dehydrocoupling:
Group 2 Mediated Boron–Nitrogen
Desilacoupling

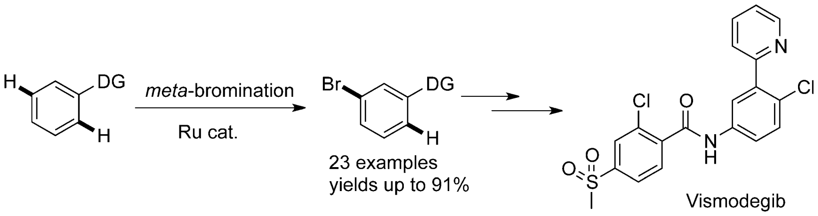

A method for direct ruthenium-catalyzed *meta*-bromination of arenes bearing various pyridyl or pyrimidyl directing groups (DGs) is reported. This procedure is demonstrated in the concise synthesis of Vismodegib, and mechanistic studies suggest that bromination proceeds through radical intermediates.

C–H Activation

Q. Yu, L. Hu, Y. Wang, S. Zheng,
J. Huang* ____ **15284 – 15288**

Directed *meta*-Selective Bromination of
Arenes with Ruthenium Catalysts

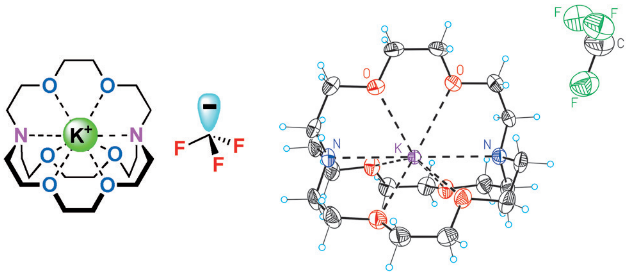

Evidence (X-ray, NMR, reactivity studies, DFT) has been obtained for the existence of the "naked" trifluoromethyl anion CF_3^-. In $[K(crypt\text{-}222)]^+ CF_3^-$, the 3D-caged potassium cation is inaccessible to CF_3^-, which makes it uncoordinated ("naked").

Carbanions

A. Lishchynskyi, F. M. Miloserdov,
E. Martin, J. Benet-Buchholz,
E. C. Escudero-Adán, A. I. Konovalov,
V. V. Grushin* ____ **15289 – 15293**

The Trifluoromethyl Anion

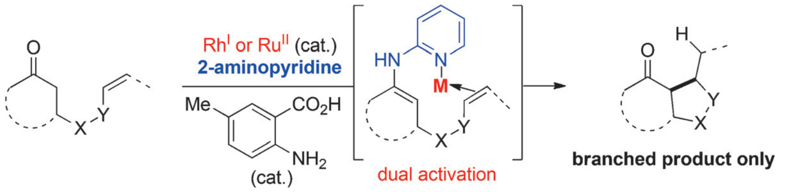

The cooperative activation of a ketone and an olefin by 2-aminopyridine and a rhodium or ruthenium catalyst leads to Conia-ene-type products with excellent regioselectivity. These transformations can be conducted under nearly pH- and redox-neutral conditions, and are thus applicable to both alkyl and aryl olefins with a broad range of functional groups.

Conia-Ene Reactions

H. N. Lim, G. Dong* ____ **15294 – 15298**

Catalytic Intramolecular Ketone Alkylation
with Olefins by Dual Activation

© 2015 Wiley-VCH Verlag GmbH & Co. KGaA, Weinheim

Supporting information is available on www.angewandte.org (see article for access details).

A video clip is available as Supporting Information on www.angewandte.org (see article for access details).

This article is available online free of charge (Open Access).

This article is accompanied by a cover picture (front or back cover, and inside or outside).

The Very Important Papers, marked VIP, have been rated unanimously as very important by the referees.

The Hot Papers are articles that the Editors have chosen on the basis of the referee reports to be of particular importance for an intensely studied area of research.

Check out these journals:

www.chemasianj.org

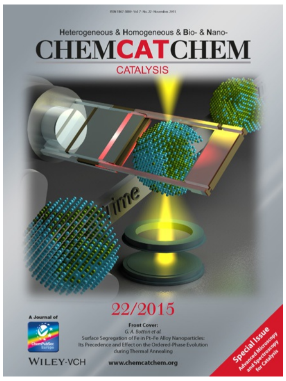

www.chemcatchem.org

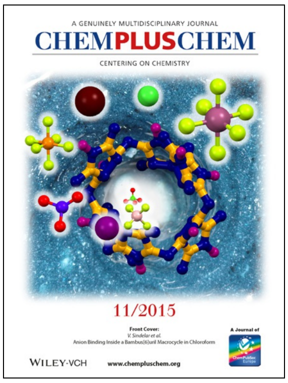

www.chempluschem.org

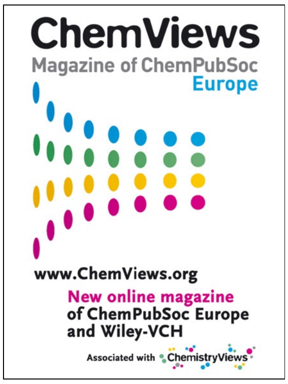

www.chemviews.org